# Evaluation of a Reverse-Tapered Design on the Osseointegration of Narrow-Diameter Implants in Beagle Dogs: A Pilot Study

Yun-Young Chang, DDS, PhD[1]/Su-Hwan Kim, DDS, PhD[2]/Keun-Oh Park, MS[3]/Jeong-Ho Yun, BS, DDS, PhD[4]

***Purpose:*** *The purpose of this study was to evaluate a reverse-tapered design on the osseointegration of narrow-diameter implants in comparison with a conventional tapered design in beagle dogs.* ***Materials and Methods:*** *All mandibular premolars and first molars were extracted bilaterally in four beagle dogs. Three months later, three kinds of implants were placed in both quadrants of the mandible: tapered narrow-diameter implants processed by cold working (TNC; n = 8), reverse-tapered narrow-diameter implants (RTN; n = 8), and reverse-tapered narrow-diameter implants processed by cold working (RTNC; n = 8). The animals were sacrificed at 4 weeks. Implant stability quotient (ISQ) values were measured at the time of implant placement and sacrifice. Histomorphometric analysis was performed.* ***Results:*** *The baseline ISQ values were significantly lower in the RTN (56.0 ± 11.6) and RTNC (57.2 ± 9.8) than in the TNC (68.0 ± 5.4; P = .021). At 4 weeks, the TNC (69.9 ± 5.1) exhibited significantly higher ISQ values compared with the RTNC (61.6 ± 4.1; P = .024). Histologic analysis in the RTN and RTNC revealed osseointegration without any signs of inflammation; however, unresolved coronal gap or dehiscence was also observed. The total bone-to-implant contact ratios (BIC) in TNC, RTN, and RTNC were 55.1% ± 11.5%, 47.8% ± 19.1%, and 60.2% ± 15.3%, respectively, and no significant differences were shown among them. The BIC for the coronal part in each group was 51.1% ± 29.4%, 28.8% ± 33.8%, and 23.9% ± 23.3%, respectively, and the differences were not significant. In the threaded part, TNC, RTN, and RTNC showed a BIC of 56.3% ± 9.6%, 50.7% ± 18.3%, and 65.3% ± 15.6%, respectively. There was no significant difference among them.* ***Conclusion:*** *The reverse-tapered design on narrow-diameter implants showed a lower initial stability than the conventional tapered design; however, there was equivalent osseointegration in an early healing phase.*
Int J Oral Maxillofac Implants 2016;31:611–620. doi: 10.11607/jomi.4260

**Keywords:** *animal, dental implant, histology, osseointegration, titanium*

[1]Periodontist, Division of Periodontology, Department of Dentistry, Inha International Medical Center, Incheon, Republic of Korea.
[2]Associate Professor, Department of Periodontics, Asan Medical Center and Department of Dentistry, University of Ulsan College of Medicine, Seoul, Republic of Korea.
[3]Researcher, Department of Bio-fibers and Materials Science, Kyungpook National University, Daegu, Republic of Korea.
[4]Associate Professor, Department of Periodontology, School of Dentistry and Institute of Oral Bioscience, Chonbuk National University, Jeonju, Republic of Korea; Research Institute of Clinical Medicine of Chonbuk National University-Biomedical Research Institute of Chonbuk National University Hospital, Jeonju, Republic of Korea.

**Correspondence to:** Dr Jeong-Ho Yun, Department of Periodontology, School of Dentistry, Chonbuk National University, 567 Baekje-daero, Deokjin-gu, Jeonju-si, Jeollabuk-do 54896, Republic of Korea.
Fax: +82-63-250-2289. Email: grayheron@hanmail.net



Narrow-diameter implants are one of the options available for implant placement on resorbed alveolar ridges without augmentation procedures. These implants may not only minimize the inevitable postoperative complications of implant surgery, but also decrease the extended healing time and cost of the augmentation procedure. Many studies have shown predictable survival and success rates of narrow-diameter implants used for the rehabilitation of edentulous areas.[1–3] However, previous studies have shown that the use of narrow-diameter implants resulted in a higher stress concentration on the alveolar crest and lower loading force distribution to the supporting bone.[4–6]

Implant design is one of the factors that affects initial stability at implant placement and crestal bone stability under loading conditions after osseointegration.[7] Among several elements that determine the implant design, thread-related features are considered critical.[8,9] The various factors associated with implant thread designs include thread height, shape, width, pitch distance,

and helix/face angle. These factors are interrelated, thus affecting the biomechanical interfacial reactions on the surrounding bone.[10]

Narrow-diameter implants with a novel design were recently developed. This new type of implant has a narrow-diameter platform design and does not possess threads on the coronal one-third. On the middle and apical one-third, this implant has a normal-tapered core, but uneven thread height of macrothreads, which means that, as the thread of the implant progresses apically, its height increases. Macroscopically, these implants are reverse-tapered, in contrast to the conventional tapered design. In other words, the profile of this novel narrow-diameter implant is similar to a trapezoidal profile because of its greater apical thread height. Also, the height and width of macrothreads are relatively higher and wider than those of conventional threads. This novel narrow-diameter implant was designed to minimize the occurrence of dehiscence defects, even on resorbed alveolar ridges, which can be attributed to the narrow core diameter. Simultaneously, bone-to-implant contact and appropriate initial stability can be sufficiently achieved on relatively less resorbed inferior cancellous areas of alveolar bone with a long thread, on the basis of the fact that alveolar bone resorption following extraction is more prominent in the crestal bone region than in the apical cancellous bone.[11] In addition, an adequate surface area for direct contact with the surrounding bone is ensured through the use of long and wide threads. A previous review[7] that investigated thread patterns to affect osseointegration stated that the higher thread height may be beneficial for obtaining adequate initial stability in poor-quality bone and resisting occlusal force, which can be contributed to the higher functional surface area in direct contact to the surrounding bone.

The purpose of this study was to investigate a reverse-tapered design on the osseointegration of narrow-diameter implants in comparison with a conventional tapered design in beagle dogs.

## MATERIALS AND METHODS

### Animals

Four male beagle dogs (Orient Bio) aged 12 months and weighing 14.5 to 15.5 kg were used in this study. All animals had a complete and healthy permanent dentition and were kept in individual stainless steel cages under standard laboratory conditions (ambient temperature, 23°C ± 3°C; relative humidity, 55% ± 15%; ventilation, 10 to 20 times/hour; 12-hour light/dark cycle; and intensity of illumination, 150 to 300 lux). Ad libitum access to water and a pelleted laboratory diet were provided to all animals. Animal selection, management, surgical preparation, and other procedures were performed according to the regulations approved by the Institutional Animal Care and Use Committee at the Korean Animal Medical Science Institute (13-KE-072). The environmental conditions, ie, temperature, humidity, ventilation, and illumination intensity were periodically checked and monitored by a trained veterinarian.

### Implant Surface and Design

Two types of implants with surfaces roughened by sandblasting and acid etching were used. Their surfaces were coated with nanostructured calcium ions. Previous studies[12,13] have described the process of incorporation of calcium ions on roughened implant surfaces in detail. Briefly, calcium ions are incorporated on the titanium surface using hydrothermal treatment. The titanium implant is treated for 24 hours with a calcium solution containing 0.2 mol/L NaOH and 2 mmol/L CaO at 180°C. Then, the treated implant is cleaned using deionized water and is air dried. Finally, the implant is sterilized using gamma-ray irradiation. Among the three implant types used in the study, the first one was a conventional, tapered, narrow-diameter implant (TNC; Mini, Megagen; 2.8-mm diameter and 8-mm length, titanium grade 4 processed by cold working; Fig 1a). This implant exhibited the classical tapered configuration (core diameter, 2.6 mm) and a homogenous thread height (0.2 mm). The second type was a reverse-tapered narrow-diameter implant (RTN) exhibiting a novel design (Megagen; 2.8-mm diameter and 8-mm length, titanium grade 4; Fig 1b). It had a normal tapered core (core diameter, 2.6 mm), but the thread height of this implant was not uniform throughout its length, unlike that in the conventional threaded implant. It exhibited a reverse-tapered macroscopic configuration. These implants could be divided into three parts based on the thread configuration: the coronal one-third, which did not show any threads; the middle one-third, where the thread originated and gradually extended in length until the beginning of the apical one-third; and the apical one-third, where the thread height decreased as it progressed to the apex. The longest thread height measured was 1.4 mm, and the external diameter, including the longest thread, was eventually 5 mm at the apical one-third. Overall, the implants possessed spiral-shaped threads, a regular pitch distance of 1.1 mm, and a thread face/helix angle of 28/6.5 degrees. The third implant was a reverse-tapered narrow-diameter implant processed by cold working (RTNC; Megagen; 2.8-mm diameter and 8-mm length, titanium grade 4 processed by cold working), with a thread design and specifications identical to those of the RTN type described earlier.

The surface topographies of the TNC, RTN, and RTNC were observed using scanning electron microscopy (S-4200, Hitachi) and compared.

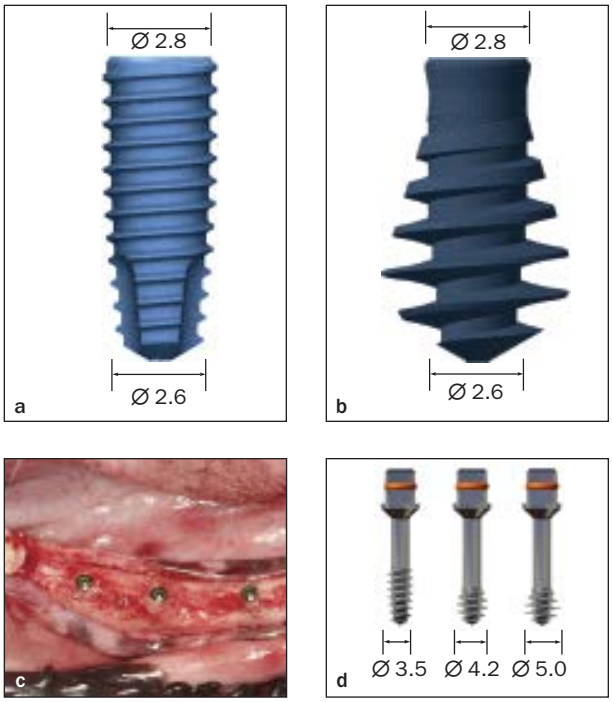


**Fig 1** *(a)* Tapered narrow-diameter implant processed by cold working (TNC; 2.8-mm diameter and 8-mm length) and *(b)* reverse-tapered narrow-diameter implant (RTN and RTNC; 2.8-mm diameter and 8-mm length). The TNC exhibits a typical tapered core with a 2.6-mm diameter and homogenous threads with a 0.2-mm height, whereas the RTN and RTNC exhibit a reverse-tapered or trapezoidal profile with wide and long threads; the core diameter was 2.6 mm, and the height of the longest thread was 1.4 mm. *(c)* Clinical photograph showing TNC, RTN, and RTNC placement. *(d)* A specially designed step-by-step tapping drill showing the first, second, and third steps with 3.5-, 4.2-, and 5-mm diameters, respectively.

## Experimental Design

Three experimental groups were formed on the basis of implant geometry and mechanical modification: the TNC group, RTN group, and RTNC group. A total of six implants, two from each group, were bilaterally placed in the mandible of each animal (three implants per quadrant). The location of implant placement was randomly assigned on the basis of a previously scheduled sequence.

## Surgical Procedure

All operative procedures were performed by an experienced surgeon (J.H.Y.) under general anesthesia and sterile conditions. All animals were allowed an adaptation period of at least 1 week in their cages before the procedure. General anesthesia was administered by the intravenous injection of 0.1 mL/kg of a solution containing equal proportions of tiletamine/zolazepam (Zoletil, Virbac) and xylazine (Rumpun, Bayer). Throughout the surgical procedure, the trained veterinarian monitored vital signs in real time. Oral prophylactic measures such as scaling and plaque control were performed 1 week before the surgical procedure. The oral cavity was disinfected using 2% povidone-iodine. Subsequently, a routine anesthetic (2% lidocaine HCl with 1:100,000 epinephrine, Kwangmyung Pharmaceutical) was locally infiltrated at the surgical sites. The mandibular first, second, third, and fourth premolars along with the first molars on both sides were carefully extracted prior to the experiment. All animals were prescribed antibiotics and nonsteroidal anti-inflammatory drugs for 5 days. After a 3-month healing period, complete healing of the extraction socket was confirmed under general anesthesia (as described previously). A midcrestal incision was placed from the canine to the second molar. A mucoperiosteal flap was bilaterally reflected, and the experimental sites were completely exposed. Three implants were randomly selected and placed in each mandibular quadrant; a total of six implants were placed in each animal (Fig 1c). Implant osteotomy was performed for TNC implants using sequential twist drills under copious saline irrigation. Implants were placed with an average insertion torque of 38.9 $\pm$ 5.1 Ncm.

The RTNs and RTNCs were placed according to the manufacturer's instructions as follows. The osteotomy steps were identical to those for TNC implants until the use of the final twist drill with a 2.8-mm diameter. Then, the first tapping drill with an external diameter of 3.5 mm was inserted into the drilled hole with a torque of 50 Ncm (Fig 1d). This was followed by the use of a second tapping drill with an external diameter of 4.2 mm and threads only in its apical half. Finally, a third tapping drill with an external diameter of 5.0 mm, which also contained threads only in its apical half, was carefully inserted with a torque of 50 Ncm. The RTNs and RTNCs were inserted into the drilled holes with an average insertion torque of 48.6 $\pm$ 7.5 and 47.4 $\pm$ 4.6 Ncm, respectively. Following implant placement, implant stability quotient (ISQ) values were measured twice with a commercially available device (Osstell Mentor, Integration Diagnostics) from the mesial and buccal directions in each implant to serve as baseline values. The mean of the ISQ values in the mesial and buccal directions was then obtained. Implants were submerged using cover screws. The mucoperiosteal flap was repositioned and sutured using 4-0 monofilamentous resorbable suture material

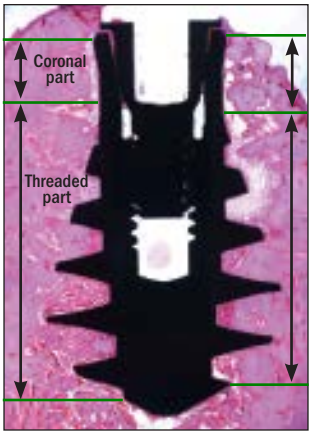


**Fig 2** Histologic image illustrating morphometric landmarks. Histometric measurements were performed by dividing the RTNs and RTNCs into two parts along the long axis: a coronal part and a threaded part. The buccal and lingual coronal parts extend from the implant shoulder to the starting point of the first thread, whereas the buccal and lingual threaded parts extend from the starting point of the first thread to the ending point of the last thread. The linear distances for the coronal parts and threaded parts in the RTN and RTNC groups, respectively, were measured, averaged, and used as a reference for dividing the coronal and threaded parts in the TNCs.

**Table 1 ISQ Values for the TNC, RTN, and RTNC at Baseline and After 4 Weeks of Healing**

| | TNC | RTN | RTNC |
|---|---|---|---|
| **Baseline** | 68.0 ± 5.4 | 56.0 ± 11.6* | 57.2 ± 9.8* |
| **4 wk** | 69.9 ± 5.1 | 63.4 ± 2.7 | 61.6 ± 4.1* |

*The difference is statistically significant when compared with the TNC group.

(Monosyn 4.0 Glyconate Monofilament, B. Braun). Antibiotics and nonsteroidal anti-inflammatory drugs were administered to all the animals for 5 days, and a canned, soft dog diet was provided 14 days after surgery. Topical dressing was performed daily until the sutures were removed on the seventh day after surgery. The surgical sites were allowed to heal for 4 weeks. Then, the animals were sacrificed by amputation of their auxiliary artery and vein under general anesthesia. At the time of sacrifice, ISQ values were measured again and recorded after exposing the cover screw only. Block sections, including the experimental sites, were dissected and fixed using 10% neutral-buffered formalin for 10 days. Prior to histologic examination, all specimen blocks were observed using microcomputed tomography (micro-CT). The specimens were scanned using a micro-CT scanner (Inveon, Siemens) with a resolution, voltage, current, and exposure time of 39 μm, 60 kV, 400 μA, and 400 ms, respectively. The charge-coupled device (CCD) readout was 3,072 × 2,048, and the number of rotation steps was 360. The region of interest was three-dimensionally reconstructed using the COBRA Exxim software program (Siemens).

## Histologic and Histometric Analysis

Resected specimens were dehydrated using ethanol, embedded in methyl-methacrylate (Technovit 7200, Kulzer) for a nondecalcified preparation, and sectioned along the buccolingual plane using a diamond saw (EXAKT cutting system 310 and micro-grinding system 400, Apparatebau). The final thickness of the cross-sectioned specimens was approximately 30 to 50 μm. They were then stained with hematoxylin-eosin (H & E). Each histologic section was analyzed using a light microscope equipped with a camera (Axioscope A1 and AxioCam HRc, Zeiss). Histometric measurements were obtained using an automated image analysis computer program (Image-Pro Plus, Media Cybernetics) by an experienced investigator (S.H.K.), who was blinded to the hypothesis of this study and its experimental groups. The investigator performed histometric measurements twice within a 2-week interval using four randomly selected sections for calibrating intraexaminer errors. For histometric analysis, the bone-to-implant contact ratio (BIC, expressed in %) was measured. The BIC was determined by calculating the percentage of actual length of the implant surface in direct contact to surrounding bone. Before measuring BIC, the implant was transversely divided into two parts along its long axis (Fig 2): *(1)* a coronal part, extending from the implant shoulder to the starting point of the first thread of the RTNs or RTNCs; and *(2)* a threaded part, extending from the starting point of the first thread to the ending point of the final thread of the RTNs or RTNCs. The BIC value for the buccal and lingual surfaces of the two parts was measured and averaged. Meanwhile, the average vertical distance of the two parts was measured, and a reference point identical to this averaged vertical distance was established in the TNC. On the basis of the reference point, the long axis of the TNC implants was also divided into a coronal part and a threaded part. In the TNC group, the BIC values were obtained using the same method employed for the RTN and RTNC groups. Meanwhile, the total BIC of the implant surface, including the coronal part and threaded part, was also calculated in all groups.

## Statistical Analysis

The statistical analysis was done using a statistical software program (SPSS 15.0, SPSS). ISQ and histometric data for each experimental group were presented as mean and standard deviation values. The Kruskal–Wallis test was performed to determine statistically significant differences among the experimental groups during the same observation period. The level of statistical significance was determined at $P < .05$, and the Tukey test was used as a post hoc test. The Wilcoxon rank-sum test was performed to compare ISQ values obtained at baseline and those obtained during the 4-week healing period.

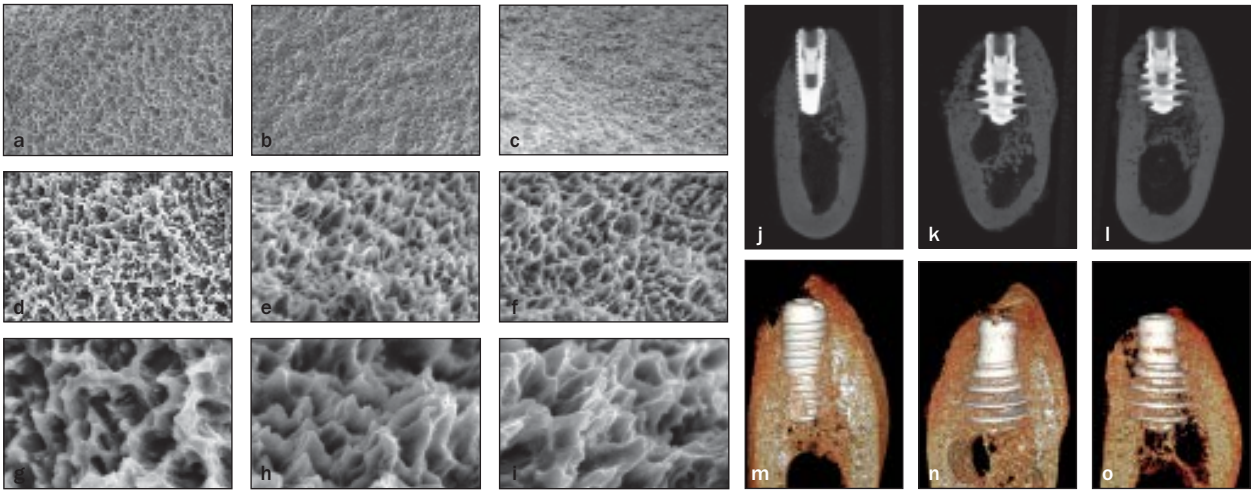


**Fig 3** Scanning electron microscope images and micro-CT view illustrating cross-sectional and three-dimensional images of *(a, d, g, j, m)* TNCs, *(b, e, h, k, n)* RTNs, and *(c, f, i, l, o)* RTNCs. Scanning electron microscope images were obtained at the original, *(a, b, c)* ×500, *(d, e, f)* ×3,000, and *(g, h, i)* ×10,000 magnifications, with no differences observed among the three groups with regard to surface morphology under each magnification. Three-dimensional reconstructed images showed that wide interthread spaces were evidently occupied by newly formed bone in the RTN and RTNC groups; the difference between both groups was not significant in this regard.

## RESULTS

### Clinical Observations

The experimental sites in all animals healed uneventfully and did not exhibit any aberrations such as wound infection, cover screw exposure, and soft tissue inflammation throughout the postoperative period. A total of 24 implants were placed in each quadrant of the mandible of four animals (TNC group [n = 8], RTN group [n = 8], and RTNC group [n = 8]). None of these implants failed.

### Resonance Frequency Analysis

The mean ISQ values are summarized in Table 1. The baseline ISQ values in TNC, RTN, and RTNC were 68.0 ± 5.4, 56.0 ± 11.6, and 57.2 ± 9.8, respectively. Significantly higher ISQ values in the TNC than in the RTN and RTNC were observed ($P = .021$). There was no significant difference between the RTN and RTNC. After a 4-week healing period, the ISQ values in TNC, RTN, and RTNC were 69.9 ± 5.1, 63.4 ± 2.7, and 61.6 ± 4.1, respectively. The TNC exhibited higher ISQ values compared with the RTN and RTNC, with a significant difference between the TNC and RTNC ($P = .024$). No significant difference was observed between the RTN and RTNC at the 4-week healing period. As the healing time increased (from baseline to 4 weeks), ISQ values in all groups increased; however, there were no significant differences.

### Surface Topography and Microcomputed Tomography

All groups showed prominent surface roughness resulting from sandblasting and acid etching, despite being coated with calcium ions. There were no differences among the three groups with regard to surface morphology under both low and high magnifications (Fig 3).

Three-dimensionally reconstructed images of TNC, RTN, and RTNC specimens are shown in Fig 3. All implants were intimately surrounded by newly formed bone, with no significant differences among implants. Meanwhile, in the RTN and RTNC groups, the presence of newly formed bone was evident in the interthread spaces, which appeared to be even greater in the cancellous region along the thread height.

### Histologic Analysis

All implants showed successful bone-to-implant contact without any signs of inflammatory infiltration. In the TNC group, newly formed immature bone was observed between the implant surface and parent bone, revealing a reversal line (Fig 4a). Interthread spaces were filled with the apposition of dense newly formed bone matrix or a thin rim of newly formed bone and bone marrow (Figs 4a and 4b). This newly formed bone matrix (osteoid) was amorphous, hypomineralized, and in direct contact with the implant surface (Fig 4c).

New bone formation was also observed along the thread of the implants in the RTN group (Fig 5a). In most specimens, the tapped space in the parent bone could be observed, from which newly formed woven bone had originated and was in direct contact with the implant surface (Figs 5b and 5c). At a higher magnification, an osteoblast lining was observed around the newly formed bone, with osteoid forming (Fig 5c). In the cancellous region, newly formed bone was also

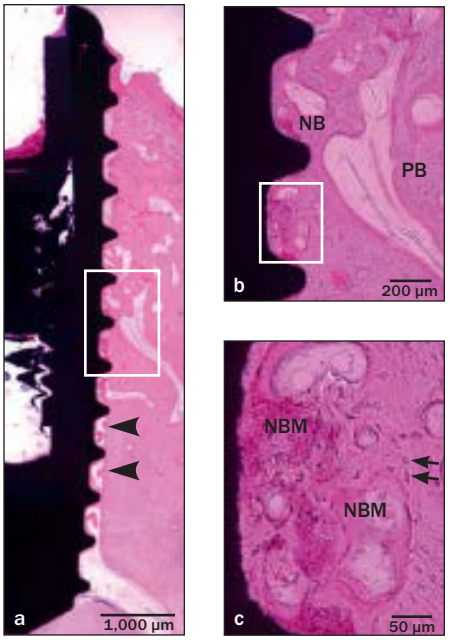


**Fig 4** *(a)* Histologic image of a TNC specimen as observed under low magnification. Newly formed bone extending from the parent bone has integrated with the implant surface, showing a reversal line *(black arrowheads). (b)* Newly formed bone and matrix (osteoid) are observed between the implant surface and parent bone. *(c)* Newly formed bone matrix is closely attached to the implant surface (H & E staining; original magnification: *a,* ×50; *b,* ×100; *c,* ×400; black arrows = osteocyte, PB = parent bone; NB = newly formed bone; NBM = newly formed bone matrix).

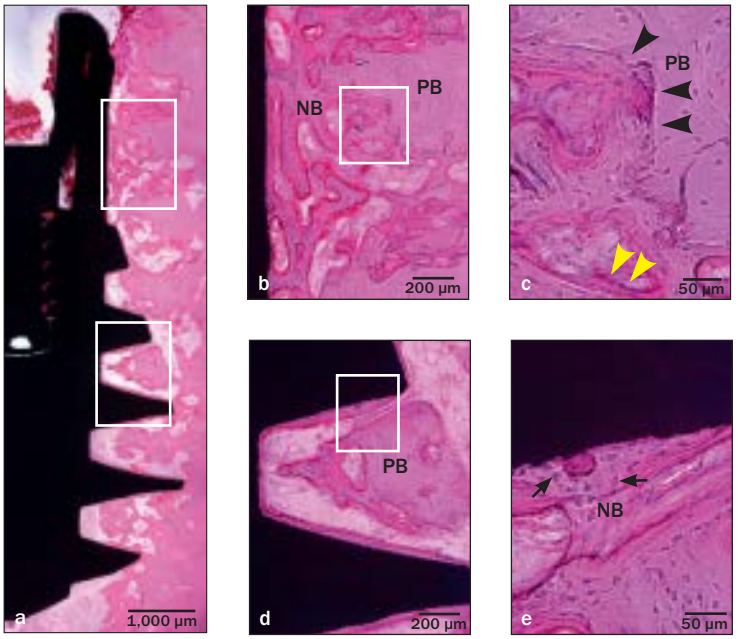


**Fig 5** *(a)* Histologic image of a RTN specimen as observed under low magnification. Signs of inflammation are not observed at the bone-implant interface. *(b)* Newly formed trabecular bone originating from the margin of tapped osteotomy has integrated with the coronal nonthreaded surface of the implant. *(c)* An osteoblastic lining *(yellow arrowheads)* can be observed around the newly formed bone. *(d)* Newly formed bone is observed along the thread in cancellous bone. *(e)* A bony bridge connecting the parent bone with the integrated, newly formed bone is observed (H & E staining; original magnification: *a,* ×50; *b* and *d,* ×100; *c* and *e,* ×400; black arrowheads = margin of tapped osteotomy; black arrows = osteocyte; NB = newly formed bone; PB = parent bone).

integrated along the thread surface, simultaneously forming a bone bridge between the newly formed bone on the threaded surface and that on the parent bone (Figs 5d and 5e). A small gap was observed in the coronal portion of the bone-implant interface in four specimens in the RTN group (Fig 6a), which exhibited connective tissue containing collagen fibers, fibroblasts, and vessels. A thin layer of dense connective tissue was attached to the implant surface of the RTN group specimens (Fig 6b).

The overall histologic features of the RTNC specimens were similar to those of the RTN specimens (Fig 7a). The apposition and ingrowth of newly formed woven bone were apparent between the parent bone and implant surface (Figs 7b and 7c). Interthread spaces as well as a tapped space in the parent bone were also occupied by newly formed bone and an amorphous osteoid (Figs 7d and 7e). In three specimens that exhibited a relatively wide tapped space, as in the RTN group, the extension of connective tissue into the gap between the tapped osteotomy margin and implant surface could be observed.

## Histometric Analysis

The findings of histometric analysis are summarized in Table 2. The vertical distance of the coronal parts in the TNC, RTN, and RTNC groups was 1.77 ± 0.02, 1.80 ± 0.08, and 1.75 ± 0.09 mm, respectively, with no significant differences among the groups. Also, there were no significant differences in the vertical distance of the threaded parts in the TNC, RTN, and RTNC groups, which was 5.63 ± 0.22, 5.43 ± 0.17, and 5.52 ± 0.30 mm, respectively.

The total BIC in the TNC, RTN, and RTNC groups was 55.1% ± 11.5%, 47.8% ± 19.1%, and 60.2% ± 15.3%, respectively, and showed no significant differences among the three groups. The BIC for the coronal part in each group was 51.1% ± 29.4%, 28.8% ± 33.8%, and 23.9% ± 23.3%, respectively, and was the highest in the TNC group; however, the differences were not significant. In the threaded part, TNC, RTN, and RTNC showed a BIC of 56.3% ± 9.6%, 50.7% ± 18.3%, and 65.3% ± 15.6%, respectively. There was no significant difference among the three groups.

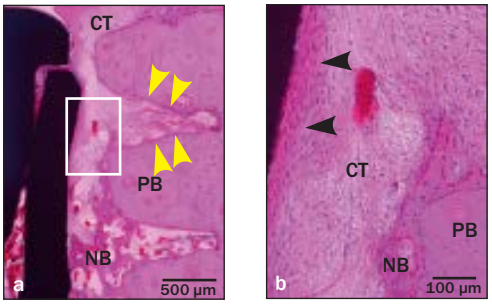


**Fig 6** *(a)* Histologic view of another RTN specimen as observed under low magnification. Cell-rich connective tissue has grown into the gap created by the tapping procedure. Newly formed bone extends from the margin of tapped osteotomy *(yellow arrowheads)* and the base of the gap defect. *(b)* Linear dense connective tissue *(black arrowheads)* has attached to the surface of the coronal part (H & E staining; original magnification: *a,* ×50; *b,* ×200; CT = connective tissue; PB = parent bone; NB = newly formed bone).

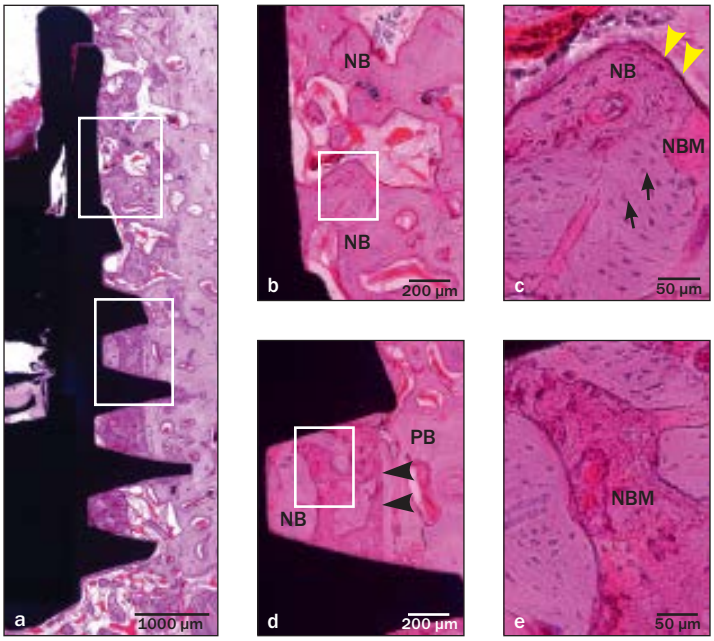


**Fig 7** *(a)* Histologic view of a RTNC specimen as observed under low magnification. *(b)* Newly formed bone has integrated with the surface of the coronal part. *(c)* Osteoblasts *(yellow arrowheads)* are also observed around the newly formed bone and matrix. *(d)* Dense newly formed bone matrix and newly formed bone occupy the interthread spaces, demarcated by a reversal line *(black arrowheads)* and thread, and have integrated with the implant surface. *(e)* Newly formed bone matrix is observed between the newly formed bone and the parent bone (H & E staining; original magnification: *a,* ×50; *b* and *d,* ×100; *c* and *e,* ×400; black arrows = osteocyte; PB = parent bone; NB = newly formed bone; NBM = newly formed bone matrix).

## DISCUSSION

The RTNs and RTNCs used in the present study differed from the conventional implants with respect to implant geometry. This distinct reverse-tapered design was primarily devised for narrow-diameter implants to enable their routine use for the rehabilitation of posterior edentulous areas. Moreover, it was aimed to restore a narrow edentulous ridge with minimized ridge augmentation. It is because of this that the narrow platform in RTN and RTNC could be more advantageous than the regular and wide platform in conventional implants for augmentation of a horizontal dehiscence defect. Previous studies that evaluated the possibility of narrow-diameter implants for rehabilitation of a posterior narrow edentulous ridge by using material modification have been reported; however, approaches in the aspect of implant design have been lacking.

Histologic examination revealed that the RTN and RTNC groups as well as the TNC group achieved bone-to-implant surface contact without any prominent inflammatory reactions. Densely packed or thin-rimmed bone that had originated from the parent bone was successfully integrated into the implant surface within just 4 weeks. The total BIC values for the RTN and RTNC groups were equivalent to those for the TNC group. This finding indicated the amount of BIC in the reverse-tapered design was equal to that in the conventional-tapered design.

**Table 2 Histometric Data in Each Group at 4 Weeks (Mean ± SD, n = 8 )**

| BIC (%) | TNC | RTN | RTNC |
|---|---|---|---|
| Total | 55.1 ± 11.5 | 47.8 ± 19.1 | 60.2 ± 15.3 |
| Coronal | 51.1 ± 29.4 | 28.8 ± 33.8 | 23.9 ± 23.3 |
| Threaded | 56.3 ± 9.6 | 50.7 ± 18.3 | 65.3 ± 15.6 |

BIC = bone-to-implant contact ratio.

Using three-dimensional finite element analysis, Petrie and Williams[14] showed that the use of a solid implant model with a 3.5-mm diameter resulted in a 3.5-fold higher strain on the crestal bone compared with a 6-mm-diameter model. Similarly, Ding et al[4] showed that, among narrow-diameter, standard, and wide-diameter implants, maximum interfacial stresses

and strains were generated around the shoulders of the narrow-diameter implants when their simulated test models were vertically/obliquely loaded. In this context, the stress distribution pattern of narrow-diameter implants should be carefully analyzed with regard to crestal bone resorption and fatigue fracture.[15–17] A wide surface contact area favors the distribution of stress generated from heavy occlusal loading.[18,19] In the present study, the RTN and RTNC groups showed total BIC equivalent to the TNC group. This means that the actual length in direct contact to bone was more in RTN and RTNC than in TNC, because all three groups showed the same BIC, and the length of implant surface was more in RTN and RTNC. In particular, the BIC in RTN and RTNC was majorly concentrated on the threaded part in cancellous bone. It appeared that the bone-to-implant contact of the threaded part in cancellous bone could facilitate more distribution of occlusal stress. Abuhussein et al[7] reported that implants with longer threads in the apical portion may distribute more stress in soft cancellous bone, which consequently decreases crestal resorption by decreasing stress concentration in the cortical bone. The authors of the present study speculate that RTN and RTNC dissipated the greater part of the occlusal load in the soft cancellous bone. However, to support these findings, further histomorphometric investigations with adequate statistical power and simulated loading investigations are required to verify the actual stress distribution pattern resulting from occlusal loading in RTNs and RTNCs.

Besides appropriate stress distribution, adequate mechanical strength to withstand occlusal forces is also crucial for narrow-diameter implants to rehabilitate the posterior edentulous ridge. Using a mechanical model, Allum et al[20] measured maximum load values in relation to the diameter, which represent the amount of load that the implant can resist until it enters the fracture phase. Consequently, narrow-diameter implants showed relatively lower maximum load values and bending moments. The cold-working process, which is one of the few methods employed to improve the mechanical strength of commercially pure titanium (grade 4), was used in the present study. It refers to the process of strengthening commercially pure titanium by inducing plastic deformation. When a metal is irreversibly deformed, dislocation defects are generated and increase in number in the metal crystal structure, which eventually enhances the mechanical property of the metal.[21,22] The manufacturers of RTNCs and TNCs released a technical report, in which the compressive strength of the one-piece implant manufactured using cold-worked titanium was significantly higher (20.46% $\pm$ 8.11%) than that of the one-piece implant manufactured using conventional titanium (Megagen Implant Institute of Science and Technology, unpublished data, 2013).

According to the histologic observations in the present study, no specific aberrant tissue reactions were observed around the RTNCs or TNCs, and both implant groups exhibited successful osseointegration. There was no significant difference in BIC and ISQ values between the RTNC and RTN groups. Scanning electron microscopy analysis also confirmed that the surface structure and morphology in the RTNC group were identical to those in the RTN group. These observations indicate that the cold-working process did not enhance healing and osseointegration; nevertheless, it did not adversely affect the biologic behavior and osseointegration of titanium. Furthermore, the process did not cause any complications in roughening or incorporating calcium ions on the titanium surface.

The coronal parts in the RTN and RTNC groups exhibited lower BIC compared with that in the TNC group, although the difference was not significant. In addition, the majority of the BIC in the RTN and RTNC groups was concentrated in the threaded part. These findings observed in the coronal parts of the RTN and RTNC groups were probably related to the structural characteristics of RTNs and RTNCs. To place the RTN and RTNM, a step-by-step tapping procedure was performed (diameter, 3.5 to 5.0 mm). It was presumed that a marginal gap was created between the implant and parent bone in a few specimens. Consequently, there was growth of connective tissue in this gap, which occurred faster than osteoblastic differentiation and proliferation. After 4 weeks of healing, the marginal gap was found to be osseointegrated; however, an unresolved gap or dehiscence was also found. However, RTN and RTNC surfaces are nanocoated with calcium ions, and the total observation period in the present study was just 4 weeks. It can be anticipated that this gap defect spontaneously resolved by distance osteogenesis, because the width of the gap between the implant and bone was mostly less than 1 mm on histologic examination (data not shown); furthermore, a surface nanocoated with calcium ions is more favorable for cell attachment and proliferation.[23] Suh et al[12] and Park et al[24] showed enhanced bone reactivity on nanostructured calcium-coated titanium surfaces, probably because the abundance of calcium ions on the titanium surface improves the activity of integrin, which is involved in osteoblast attachment. Botticelli et al[25] evaluated appositional bone growth in intentionally created marginal defects around implants in dogs. After a 4-week healing period, they observed limited bone formation, limited bone-to-implant contact, and dense connective tissue ingrowth. However,

bone formation and bone-to-implant contact gradually increased with progress in healing.

In the present study, resonance frequency analysis was performed to assess implant stability at the time of implant placement and the 4-week healing period. Resonance frequency analysis evaluates the stiffness of the bone-implant interface.[26,27] The baseline ISQ values for the RTN and RTNC groups were significantly lower than those for the TNC group, with no significant differences between the RTN and RTNC groups. The initial stability of RTNs and RTNCs was mainly derived from cancellous bone using long and wide threads, probably because the coronal portions of RTNs and RTNCs do not have threads, resulting in lower contact or mechanical interlocking with dense cortical bone compared with that in the TNC implants. Previous literature has revealed that the stiffness of the bone-implant interface is higher in dense bone and vice versa.[28,29] In a simulated model study, the ISQ value was reported to be significantly affected by implant-bone contact in the coronal portion.[30] The authors of the present study speculate that the peri-implant gap during RTN and RTNC placement was associated, to a certain extent, with low ISQ values.[31,32] However, an important fact to be noted was that the RTN and RTNC groups exhibited increased ISQ values after the 4-week healing period, even if the differences between values at baseline and those after the 4-week healing period were not significant. This finding indicated that newly formed bone integrated to the implant surface increased and underwent further remodeling and mineralization as the healing time increased. As a result, enhanced mechanical anchorage to the supporting bone was observed, which resulted in increased ISQ values in the RTN and RTNC groups.[33,34]

This pilot study has certain limitations. First, the sample size was small. To the best of the authors' knowledge, this is the first study evaluating the reverse-tapered design for narrow-diameter implants. This study preferentially focused on the early bone response around the TNCs, RTNs, and RTNCs, and the number of animals was determined by following animal research guidelines pertaining to the use of minimum number of animals.[35] Future long-term comparative studies with a large sample size should be performed to support the results of the present study. The findings of this pilot study were that the initial stability of RTN and RTNC was relatively low at the time of implant placement; however, it increased by secondary stability to a normal range. The RTN and RTNC showed the same amount of BIC to TNC; however, they also exhibited an unresolved coronal gap or dehiscence as well as intact coronal osseointegration.

## CONCLUSIONS

Within the limitations of this study, the results suggest that a reverse-tapered design on a narrow-diameter implant showed a lower initial stability than a conventional tapered design; however, there was equivalent osseointegration in the early healing phases.

## ACKNOWLEDGMENTS

This work was supported by the Industrial Strategic Technology Development Program (10044976) funded by the Ministry of Trade, Industry & Energy (MOTIE, Korea). The authors reported no conflicts of interest related to this study.

## REFERENCES

1. Romeo E, Lops D, Amorfini L, et al. Clinical and radiographic evaluation of small-diameter (3.3-mm) implants followed for 1-7 years: A longitudinal study. Clin Oral Implants Res 2006;17:139–148.
2. Vigolo P, Givani A, Majzoub Z, Cordioli G. Clinical evaluation of small-diameter implants in single-tooth and multiple-implant restorations: A 7-year retrospective study. Int J Oral Maxillofac Implants 2004;19:703–709.
3. Zinsli B, Sägesser T, Mericske E, Mericske-Stern R. Clinical evaluation of small-diameter ITI implants: A prospective study. Int J Oral Maxillofac Implants 2004;19:92–99.
4. Ding X, Liao SH, Zhu XH, Zhang XH, Zhang L. Effect of diameter and length on stress distribution of the alveolar crest around immediate loading implants. Clin Implant Dent Relat Res 2009;11:279–287.
5. Tada S, Stegaroiu R, Kitamura E, Miyakawa O, Kusakari H. Influence of implant design and bone quality on stress/strain distribution in bone around implants: A 3-dimensional finite element analysis. Int J Oral Maxillofac Implants 2003;18:357–368.
6. Qian L, Todo M, Matsushita Y, Koyano K. Effects of implant diameter, insertion depth, and loading angle on stress/strain fields in implant/jawbone systems: Finite element analysis. Int J Oral Maxillofac Implants 2009;24:877–886.
7. Abuhussein H, Pagni G, Rebaudi A, Wang HL. The effect of thread pattern upon implant osseointegration. Clin Oral Implants Res 2010;21:129–136.
8. Hansson S, Werke M. The implant thread as a retention element in cortical bone: The effect of thread size and thread profile: A finite element study. J Biomech 2003;36:1247–1258.
9. Huang HL, Hsu JT, Fuh LJ, et al. Bone stress and interfacial sliding analysis of implant designs on an immediately loaded maxillary implant: A non-linear finite element study. J Dent 2008;36:409–417.
10. Ausiello P, Franciosa P, Martorelli M, Watts DC. Effects of thread features in osseo-integrated titanium implants using a statistics-based finite element method. Dent Mater 2012;28:919–927.
11. Schropp L, Wenzel A, Kostopoulos L, Karring T. Bone healing and soft tissue contour changes following single-tooth extraction: A clinical and radiographic 12-month prospective study. Int J Periodontics Restorative Dent 2003;23:313–323.
12. Suh JY, Jeung OC, Choi BJ, Park JW. Effects of a novel calcium titanate coating on the osseointegration of blasted endosseous implants in rabbit tibiae. Clin Oral Implants Res 2007;18:362–369.
13. Park JW, Jang IS, Suh JY. Bone response to endosseous titanium implants surface-modified by blasting and chemical treatment: A histomorphometric study in the rabbit femur. J Biomed Mater Res B Appl Biomater 2008;84:400–407.
14. Petrie CS, Williams JL. Comparative evaluation of implant designs: Influence of diameter, length, and taper on strains in the alveolar crest. A three-dimensional finite-element analysis. Clin Oral Implants Res 2005;16:486–494.

15. Quek CE, Tan KB, Nicholls JI. Load fatigue performance of a single-tooth implant abutment system: Effect of diameter. Int J Oral Maxillofac Implants 2006;21:929–936.
16. Esposito M, Thomsen P, Ericson LE, Sennerby L, Lekholm U. Histopathologic observations on late oral implant failures. Clin Implant Dent Relat Res 2000;2:18–32.
17. Isidor F. Loss of osseointegration caused by occlusal load of oral implants. A clinical and radiographic study in monkeys. Clin Oral Implants Res 1996;7:143–152.
18. Orsini E, Giavaresi G, Trirè A, Ottani V, Salgarello S. Dental implant thread pitch and its influence on the osseointegration process: An in vivo comparison study. Int J Oral Maxillofac Implants 2012;27:383–392.
19. Lee CC, Lin SC, Kang MJ, Wu SW, Fu PY. Effects of implant threads on the contact area and stress distribution. J Dent Sci 2010;5:156–165.
20. Allum SR, Tomlinson RA, Joshi R. The impact of loads on standard diameter, small diameter and mini implants: A comparative laboratory study. Clin Oral Implants Res 2008;19:553–559.
21. Degarmo EP, Black JT, Kohser RA. Materials and Process in Manufacturing. 9th ed: John Wiley & Sons, Inc, 2003:159–172.
22. Bozzolo N, Dewobroto N, Wenk HR, Wagner F. Microstructure and microtexture of highly cold-rolled commercially pure titanium. J Mater Sci 2007;42:2405–2416.
23. Lee SY, Yang DJ, Yeo S, et al. The cytocompatibility and osseointegration of the Ti implants with XPEED surfaces. Clin Oral Implants Res 2012;23:1283–1289.
24. Park JW, Park KB, Suh JY. Effects of calcium ion incorporation on bone healing of Ti6Al4V alloy implants in rabbit tibiae. Biomaterials 2007;28:3306–3313.
25. Botticelli D, Berglundh T, Buser D, Lindhe J. Appositional bone formation in marginal defects at implants. Clin Oral Implants Res 2003;14:1–9.
26. Meredith N, Alleyne D, Cawley P. Quantitative determination of the stability of the implant-tissue interface using resonance frequency analysis. Clin Oral Implants Res 1996;7:261–267.
27. Meredith N, Book K, Friberg B, Jemt T, Sennerby L. Resonance frequency measurements of implant stability in vivo. A cross-sectional and longitudinal study of resonance frequency measurements on implants in the edentulous and partially dentate maxilla. Clin Oral Implants Res 1997;8:226–233.
28. Friberg B, Sennerby L, Meredith N, Lekholm U. A comparison between cutting torque and resonance frequency measurements of maxillary implants. A 20-month clinical study. Int J Oral Maxillofac Surg 1999;28:297–303.
29. Sennerby L, Andersson P, Verrocchi D, Viinamäki R. One-year outcomes of Neoss bimodal implants. A prospective clinical, radiographic, and RFA study. Clin Implant Dent Relat Res 2012;14:313–320.
30. Ito Y, Sato D, Yoneda S, et al. Relevance of resonance frequency analysis to evaluate dental implant stability: Simulation and histomorphometrical animal experiments. Clin Oral Implants Res 2008;19:9–14.
31. Turkyilmaz I, Sennerby L, Tumer C, Yenigul M, Avci M. Stability and marginal bone level measurements of unsplinted implants used for mandibular overdentures: A 1-year randomized prospective clinical study comparing early and conventional loading protocols. Clin Oral Implants Res 2006;17:501–505.
32. Turkyilmaz I, Sennerby L, Yilmaz B, Bilecenoglu B, Ozbek EN. Influence of defect depth on resonance frequency analysis and insertion torque values for implants placed in fresh extraction sockets: A human cadaver study. Clin Implant Dent Relat Res 2009;11:52–58.
33. Nedir R, Bischof M, Szmukler-Moncler S, Bernard JP, Samson J. Predicting osseointegration by means of implant primary stability. Clin Oral Implants Res 2004;15:520–528.
34. Becker W, Sennerby L, Bedrossian E, Becker BE, Lucchini JP. Implant stability measurements for implants placed at the time of extraction: A cohort, prospective clinical trial. J Periodontol 2005;76:391–397.
35. Kilkenny C, Browne W, Cuthill IC, Emerson M, Altman DG. Animal research: Reporting in vivo experiments: The ARRIVE guidelines. Br J Pharmacol 2010;160:1577–1579.